Electronic supplementary materials *Mendeleev Commun.*, 2013, **23**, 334−336

Redox properties and radical anions of 2-substituted thioxanthen-9-ones and its 2-methyl *S*-oxide derivatives

Nadezhda V. Vasilieva, Irina G. Irtegova, Vladimir A. Loskutov and Leonid A. Shundrin

1. Cyclic voltammograms of **1a-c** and EPR spectra of the corresponding RAs.

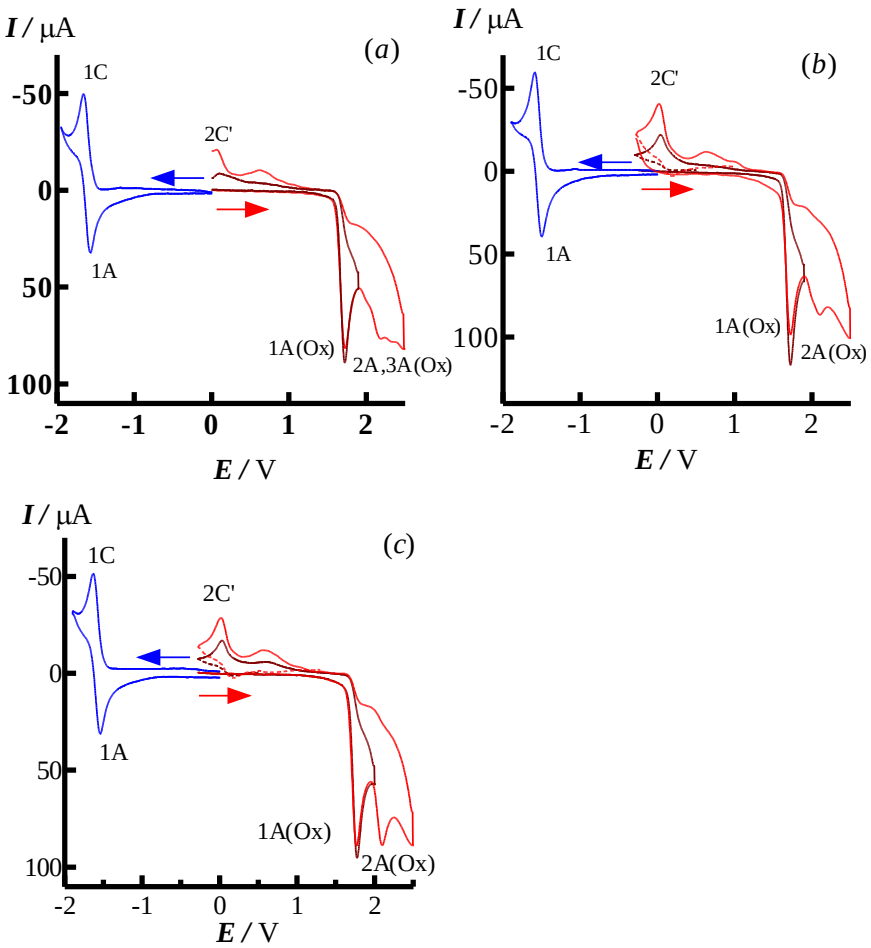

Figure S1 CV of **1a** (*a*), **1b** (b), **1c** (*c*) in MeCN within potential sweep regions: 0>E>–2.0 V (——), 2.5>E>–0.3 V (——), 2.0>E>–0.3 V (——), (ν=0.1 V·s^{-1}). *The second cycles within corresponding potential sweep ranges are indicated as* (– – –) *and* (– – –). *The beginning and direction of potential sweep are indicated by arrows.*

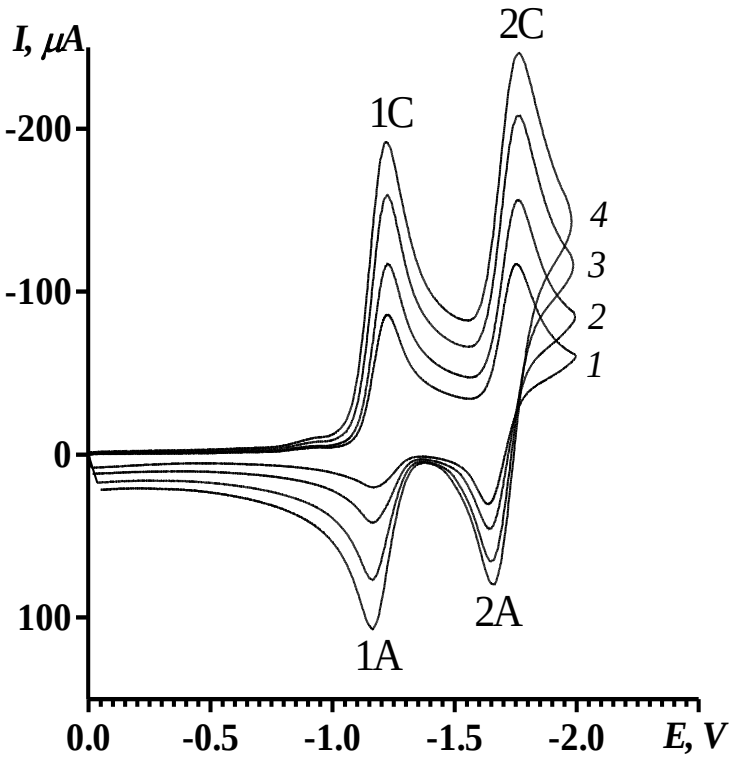

Figure S2 CV of **2** in MeCN within potential sweep regions: 0.0>E>–2.0 V at various scan rates (v = 0.1 (*1*), 0.4 (*2*), 0.8 (*3*), 1.2 (*4*) V·s^{-1})

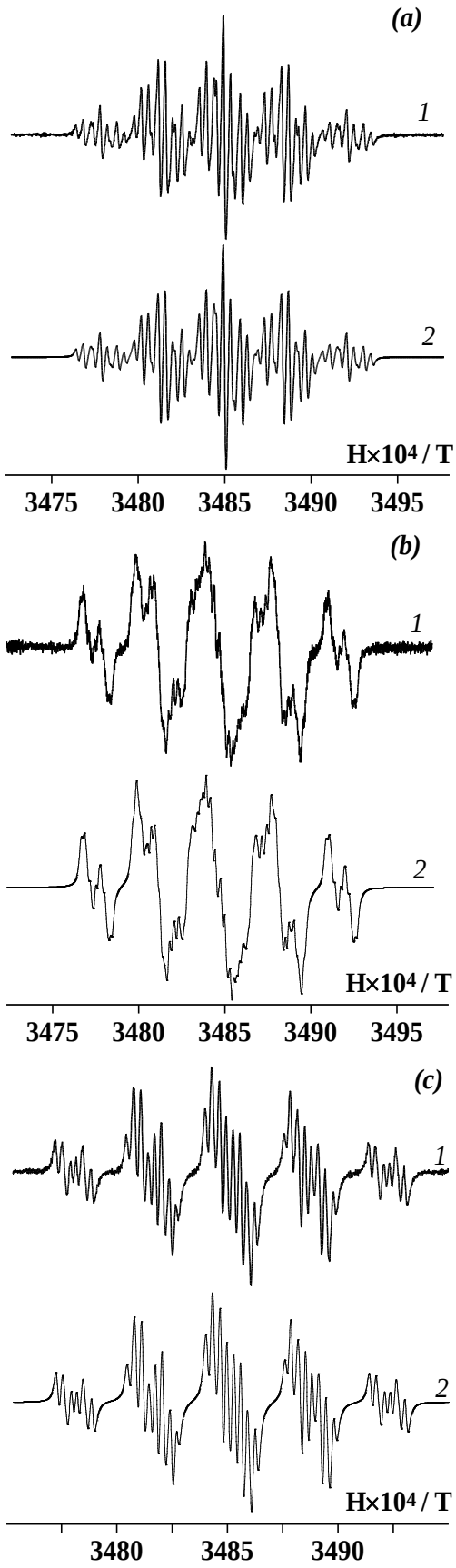

Figure S3 EPR spectra of RAs **1a-c** in MeCN (*a*, *b*, *c*, respectively). *1 – experimental spectrum, 2 – simulated spectrum.*

Table S1 Experimental redox potentials[a] of **1−3** in MeCN.

Compound	R	E_p^{1C} / V	E_p^{2C} / V	$E_p^{1A(Ox)}$ / V	$E_p^{2A(Ox)}$ / V	$E_p^{3A(Ox)}$ /V	$I_p^{1A(Ox)} / I_p^{1C}$
1a	H	–1.64	—[b]	1.71	1.99	2.16	1.84
1b	Cl	–1.57	—	1.71	2.00	2.10	2.09
1c	CO-Pr^i	–1.62	—	1.76	2.09	—	1.82
1d	Me	–1.70	—	1.62	2.09	—	2.05
2	Me	–1.24	–1.76	2.09	—	—	2.00
3	Me	–1.12	–1.71	—	—	—	—

[a] Peak potentials are listed as E_p^{iC}, E_p^{iA} and $E_p^{iA(Ox)}$ where *i* is a number of peak at CV curve, symbols C or A indicate the cathodic or anodic branch of the CV curve in reductive potentials area, A(Ox) indicates the anodic branch of the CV curve in oxidative potentials area. Potential sweep rate is 0.1 V·s^{-1}.

[b] Second peak 2C is not observed for **1a-d**.

Table S2 g-Factors and experimental ^{1}H HFCC (mT) of radical anions **1-3** together with those calculated at the UB3LYP/6-31+G* level of theory in gas phase.

RA	Experimental	UB3LYP/6-31+G*	g-factor
1a	0.337 (1,8)[a], 0.098 (2,7), 0.376 (3,6), 0.040 (4,5)	–0.391 (1,8), 0.125 (2,7), –0.434 (3,6), 0.003 (4,5)	2.0018
1b	0.371 (1), 0.428 (3), 0.020 (4), 0.036 (5), 0.323 (6), 0.084 (7), 0.300 (8), 0.010 (Cl)	–0.425 (1), –0.495 (3), –0.026 (4), 0.001 (5), –0.380 (6), 0.115 (7), –0.360 (8), –0.004 (Cl)	2.0018
1c	0.359 (1), 0.383 (3), 0.027 (4), 0.040 (5), 0.354 (6), 0.092 (7), 0.321 (8)	–0.313 (1), –0.551 (3), 0.048 (4), 0.009 (5), –0.363 (6), 0.109 (7), –0.337 (8), –0.003 (CH), –0.004 (Me)[b]	2.0019
1d	0.332 (1), 0.377 (3), 0.039 (4), 0.042 (5), 0.371 (6), 0.100 (7), 0.337 (8), 0.094 (Me)[b]	–0.370 (1), –0.463 (3), 0.002 (4), –0.008 (5), –0.410 (6), 0.121 (7), –0.383 (8), –0.116 (Me)[b]	2.0016
2	0.190 (1), 0.301 (3), 0.070 (4), 0.074 (5), 0.277 (6), 0.025 (7), 0.194 (8), 0.023 (Me)[b]	–0.233 (1), –0.370 (3), 0.100 (4), 0.100 (5), –0.364 (6), 0.073 (7), –0.238 (8), –0.061 (Me)[b]	2.0016
3[c]	0.189 (1), 0.300 (3), 0.074 (4), 0.078 (5), 0.278 (6), 0.027 (7), 0.194 (8), 0.026 (Me)[b]	–0.187 (1), –0.327 (3), 0.104 (4), 0.107 (5), –0.335 (6), 0.028 (7), –0.186 (8), –0.022 (Me)[b]	2.0064

[a] Positions of ^{1}H nuclei are shown in brackets.

[b] Averaged values in accordance with the scheme of the rapid three-jump proton exchange.

Table S3 Lowdin charges in radical anions of **1(a-d)-3** calculated at the UB3LYP/6-31+G* level of theory in gas phase.

RA	C(1) – C(9), C(11) – C(14)	O(C=O), S(10), O(S=O)
1a	−0.224, −0.250, −0.288, −0.275, −0.275, −0.288, −0.250, −0.224, +0.054, −0.089, −0.222, −0.222, −0.089	−0.536, +0.342
1b	−0.229, −0.172, −0.292, −0.264, −0.273, −0.276, −0.248, −0.220, +0.059, −0.083, −0.221, −0.222, −0.084	−0.523, +0.358
1c	−0.147, −0.119, −0.280, −0.259, −0.270, −0.276, −0.246, −0.217, +0.062, −0.090, −0.216, −0.225, −0.084	−0.510, +0.361
1d	−0.232, −0.125, −0.292, −0.264, −0.273, −0.276, −0.248, −0.220, +0.059, −0.083, −0.221, −0.222, −0.084	−0.533, +0.349
2	−0.217, −0.116, −0.284, −0.216, −0.224, −0.277, −0.240, −0.209, +0.056, −0.072, −0.273, −0.271, −0.076	−0.514, +1.012, −0.835
3	−0.209, −0.112, −0.277, −0.190, −0.198, −0.270, −0.237, −0.201, +0.066, −0.065, −0.255, −0.254, −0.071	−0.496, +1.427, −0.738, −0.700

Positions of atoms listed in Table **S2** are the following:

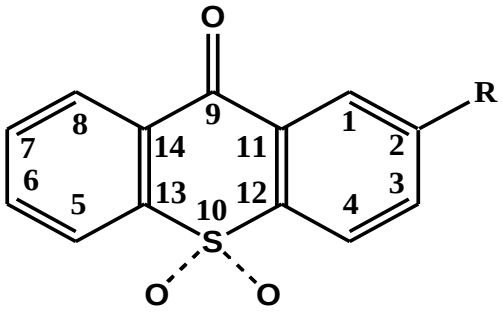

2. Digital simulation details for CV of **1d** in oxidative potentials area.

2.1. Scheme of reactions

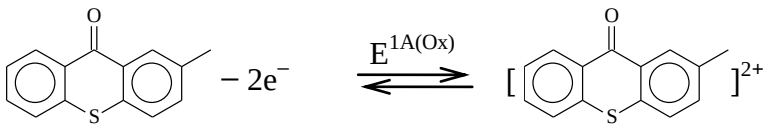

(1)

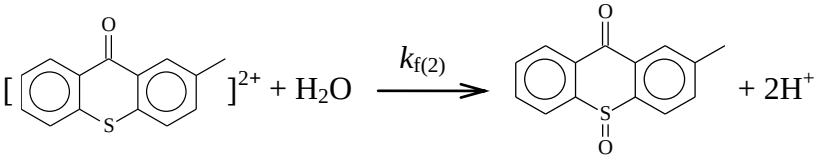

(2)

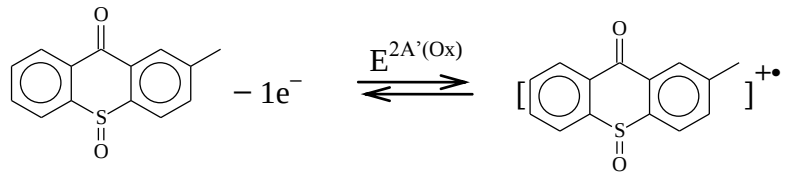

(3)

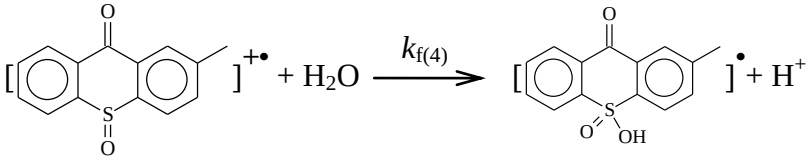

(4)

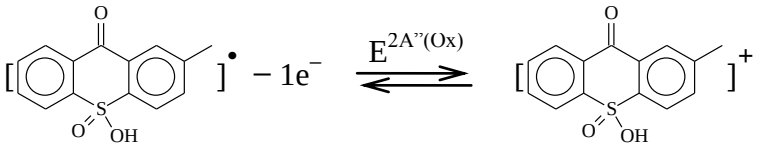

(5)

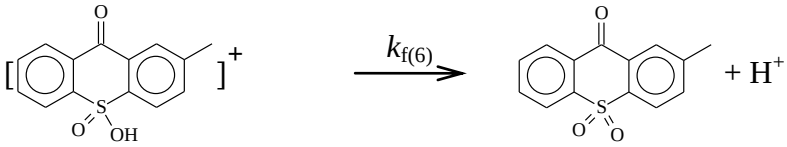

(6)

2.2. Parameters.

Fixed parameters are the following: initial concentration of depolarizer **1d** was 2.0 mM, the value of diffusion coefficient was applied as $1 \cdot 10^{-5}$ $cm^2 \cdot s^{-1}$, k_e = 0.1 $cm \cdot s^{-1}$, α = 0.5, (k_e – heterogeneous rate constant, α – transfer coefficient) for all electrochemical reactions. Water content in solution was found to be 5 mM, scan rate is 0.1 $V \cdot s^{-1}$, step time is 100 ms, initial and final potentials are –0.303 V, vertex potential is +2.507 V. i-R compensation used for simulation: R = 180 Ω, T = 293 K. Pure resistance (R) of electrochemical cell has been measured using LCR meter INSTEK (Taiwan) with signal frequency of 1kHz and amplitude of 0.5 V.

The potentials of 1A(Ox), 2A'(Ox), 2A''(Ox) peaks and rate constants of non-electrochemical homogeneous reactions 2, 4, 6 were optimized. Optimized potentials are: $E^{1A(Ox)}$ = 1.602±0.010 V, $E^{2A'(Ox)}$ = 2.026±0.012 V, $E^{2A''(Ox)}$ = 2.035±0.015 V. The following optimized rate constants for irreversible homogeneous reactions 2, 4, 6 were found: $k_{f(2)}$=(9.20±0.35)·10^3 $M^{-1} \cdot s^{-1}$, $k_{f(4)}$=(2.39±0.52)·10^3 $M^{-1} \cdot s^{-1}$ and $k_{f(6)}$= 2.22±0.55 s^{-1}.

3. Comparison of possible routes of the electrochemical oxidation of **2**.

Electrochemical oxidation of 2-methylthioxanthen-9-one sulfoxide (**2**) (Figure 2 (*b*), (*c*), see main text) can be proceed by two routes: the first one is described by reactions (3-6) (**2.1**. Scheme of reactions), the second one represents hypothetical disproportionation mechanism,

which includes one-electron electrochemical stage (7), radical cation coupling reaction(8), irreversible disproportionation stage (9) and water addition (10) (Figure **S4**).

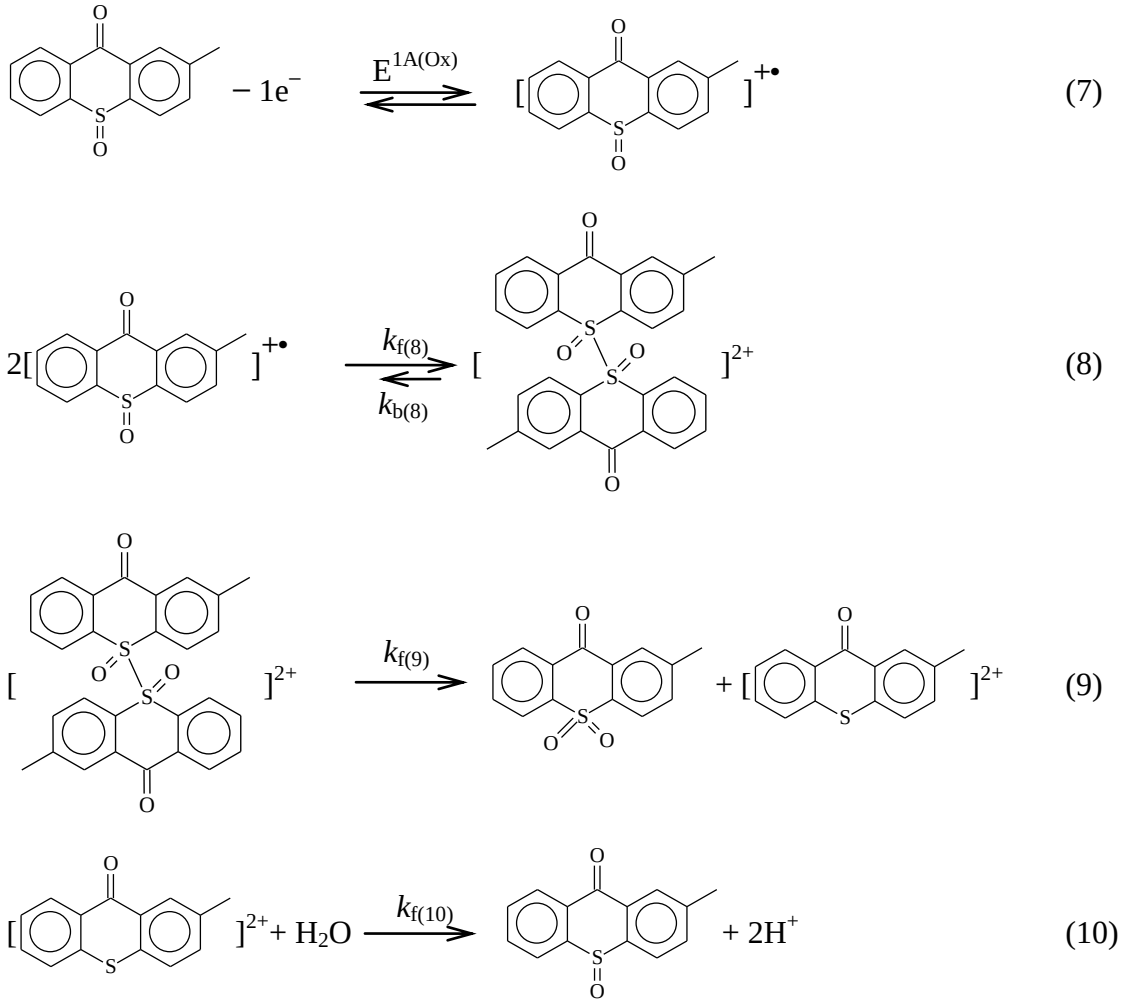

Figure **S4**. Disproportionation mechanism of ECO of **2**.

Experimental and simulated CVs of **2** within potential range −1.4>E>2.3 V (vs. s.c.e) are shown in Fig. **S5**. One electron reversible electrochemical reductions of **2** (peaks 1C, 1A, Fig. **S5**) and **3** are included into consideration as a reference. Sulfone **3** is formed from ECO of **2** (9) and has electrochemical reduction potential close to **2** (see main text). Minor reduction process, which results in the appearance of 2C' peak at the cathode branch of CV has not been included into consideration (see main text).

Rate constants of non-electrochemical homogeneous reactions, used for CV simulations are summarized in Table **S4**. The best coincidence of experimental and simulated data was obtained for two electron ECO of **2** according to the reactions 3-6 (Figure **S5** (*a*)). If the disproportionation mechanism was proposed, the best fitting was achieved for $k_{f(8)}$ =8.387·10^4 M^{-1} s^{-1} (Figure **S5**, (*b*), curve *1*), which is 29.4 times more than the constant of nucleophilic addition (H_2O in our case) to the radical cation of **2** in accordance with simulation data.

Simulated oxidative peak has a lesser width than the corresponding peak in previous case, because the only electrochemical reaction is involved into consideration.

Table **S4** Rate constants of not electrochemical homogeneous reactions used for CV simulations of ECO of **2**.

Curve*	$k_{f(4)}\times10^{-3}$, $M^{-1}s^{-1}$	$k_{f(6)}$, s^{-1}	$k_{f(8)}\times10^{-3}$, $M^{-1}s^{-1}$	$k_{b(8)}$, s^{-1}	$k_{f(9)}$, s^{-1}	$k_{f(10)}\times10^{-3}$, $M^{-1}s^{-1}$
(*a*), *1*	***2.85***	***2.55***	—	—	—	—
(*b*), *1*	—	—	***83.87***	500	$1\ 10^3$	***7.87***
(*b*), *2*	—	—	7.87	49.2	$1\ 10^3$	7.87
(*b*), *3*	—	—	1.0	5.96	$1\ 10^3$	7.87

* - as indicated in Figure **S5**.
- optimized rate constants are indicated by ***bold italic*.

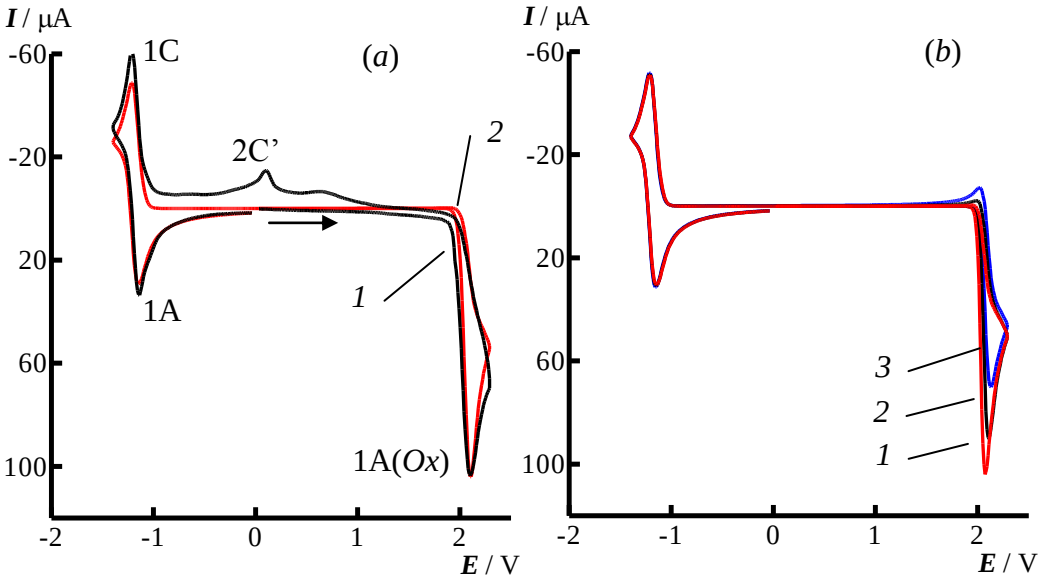

Figure **S5**. Experimental ((*a*), *1*) and simulated cyclic voltammograms of **2** within potential sweep range –1.4>E>2.3 V: (*a*), *2* – two-electron ECO of **2** in accordance with the reactions (3-6); (*b*), 1-3 – ECO of **2** in accordance with the reactions (7-10) with various rate constants (Table **S4**). *An arrow indicates the beginning and direction of potential sweep*.

The problem of competition between radical-radical and radical-substrate coupling mechanisms has been discussed by V.D. Parker [1], who has concluded that radical ion-substrate coupling is preferable as compared with radical-radical dimerization from the kinetic point of view. Typical rate constants for the latter process are less than those for radical ion-substrate reactions [1]. In

our case this situation was simulated by curve *3* (Figure **S5**, (*b*)), which differs from the experimental curve to the utmost.

The case of ECO of **2** is quite differ from the ECO of unsubstituted thioxantene [2], for which the linked by S-S bond product of the radical-radical coupling reaction was observed. We would like to note, that the value of $k_{f(8)}$ (~10^4 $M^{-1}s^{-1}$), which greatly exceeds $k_{f(4),}$ is less probable due to the steric reasons, because sulfur atom is coupled with oxygen atom in radical cation of **2**.

Thus, digital simulations of the CV curve of **2** indicate the preference of two-electron mechanism of ECO as compared with disproportionation.

References

1 V. D. Parker, *Acta Chem. Scand.*, 1998, **52**, 154.

2 P. T. Kissinger, P. T. Holt, and C. N. Reilley, *J. Electroanal. Chem.*, 1971, **33,** 1.